REPORT DOCUMENTATION PAGE

Form Approved
OMB No. 0704-0188

1. REPORT DATE *(DD-MM-YYYY)*	**2. REPORT TYPE**	**3. DATES COVERED** *(From - To)*
13-10-2009	Technical Paper	

4. TITLE AND SUBTITLE

On the Impact of Injection Schemes on Transition in Hypersonic Boundary Layers

5a. CONTRACT NUMBER

5b. GRANT NUMBER

5c. PROGRAM ELEMENT NUMBER

6. AUTHOR(S)
Ivett A. Leyva (AFRL/RZSA), Joseph S. Jewell, Stuart Laurence, Hans G. Hornung, and Joe Shepherd (CalTech)

5d. PROJECT NUMBER

5e. TASK NUMBER

5f. WORK UNIT NUMBER
23070725

7. PERFORMING ORGANIZATION NAME(S) AND ADDRESS(ES)

Air Force Research Laboratory (AFMC)
AFRL/RZST
4 Draco Drive
Edwards AFB CA 93524-7160

8. PERFORMING ORGANIZATION REPORT NUMBER

AFRL-RZ-ED-TP-2009-366

9. SPONSORING / MONITORING AGENCY NAME(S) AND ADDRESS(ES)

Air Force Research Laboratory (AFMC)
AFRL/RZS
5 Pollux Drive
Edwards AFB CA 93524-7048

10. SPONSOR/MONITOR'S ACRONYM(S)

11. SPONSOR/MONITOR'S NUMBER(S)
AFRL-RZ-ED-TP-2009-366

12. DISTRIBUTION / AVAILABILITY STATEMENT

Approved for public release; distribution unlimited (PA #09430).

13. SUPPLEMENTARY NOTES
For 16th AIAA/DLR/DGLR International Space Planes and Hypersonic Systems and Technology Conference.

14. ABSTRACT

Three geometries are explored for injecting CO2 into the boundary layer of a sharp five degree half-angle cone. The impact of the injection geometry, namely discrete injection holes or a porous conical section, on tripping the boundary layer is examined, both with and without injected flow. The experiments are conducted at Caltech's T5 reflected shock tunnel. Two different air free-stream conditions are explored. For the discrete-hole injectors, the diameter for the injection holes is 0.75 mm nominally and the length to diameter ratio is about 30. One injector has a single row of holes and the other has four rows. With the 4-row geometry fully turbulent heat transfer values are measured within four centimeters of the last injection row for both free-stream conditions. The 1-row injector results on a reduction of 50% in the transition Reynolds number. The porous injector does not move the transition Reynolds number upstream by itself with no injection flow.

15. SUBJECT TERMS

16. SECURITY CLASSIFICATION OF:			**17. LIMITATION OF ABSTRACT**	**18. NUMBER OF PAGES**	**19a. NAME OF RESPONSIBLE PERSON**
					Ivett Leyva
a. REPORT	**b. ABSTRACT**	**c. THIS PAGE**	SAR	12	**19b. TELEPHONE NUMBER** *(include area code)*
Unclassified	**Unclassified**	**Unclassified**			N/A

On the impact of injection schemes on transition in hypersonic boundary layers

Ivett A Leyva[1],
Air Force Research Laboratory, Edwards AFB, Ca, 93536

Joseph S. Jewell[2], Stuart Laurence [3], Hans G. Hornung[4], Joe Shepherd[5]
Caltech, Pasadena, Ca, 91125

Three geometries are explored for injecting CO_2 into the boundary layer of a sharp five degree half-angle cone. The impact of the injection geometry, namely discrete injection holes or a porous conical section, on tripping the boundary layer is examined, both with and without injected flow. The experiments are conducted at Caltech's T5 reflected shock tunnel. Two different air free-stream conditions are explored. For the discrete-hole injectors, the diameter for the injection holes is 0.75 mm nominally and the length to diameter ratio is about 30. One injector has a single row of holes and the other has four rows. With the 4-row geometry fully turbulent heat transfer values are measured within four centimeters of the last injection row for both free-stream conditions. The 1-row injector results on a reduction of 50% in the transition Reynolds number. The porous injector does not move the transition Reynolds number upstream by itself with no injection flow.

Nomenclature

k	=	trip height
δ	=	boundary layer thickness
δ^*	=	boundary layer displacement thickness
Subscripts		
o	=	stagnation
e	=	edge
∞	=	free-stream

I. Introduction

Designers of scramjet engines prefer to have turbulent flow at the entrance to the engine inlet for several reasons, including reduced susceptibility to flow separation inside the engine and improved fuel mixing and mass capture [1]. While transition to turbulence occurs naturally on a full-scale vehicle, it is more difficult to ensure turbulent flow at the entrance to the inlet in a sub-scale model due to its reduced size [1]. Therefore a considerable amount of work has been done to examine different passive and active trip schemes for this application [1-4]. Berry et al. [1] examined many active or blowing trip configurations on a 33% scale Hyper-X forebody model, including a single small hole (d=0.254mm), single to triple rows with holes of the same size and 3.2 mm spacing, a single row

[1] Lead, Combustion Devices Group, AFRL/RZSA, Edwards AFB, CA, AIAA Senior Member.
[2] Graduate Student, Caltech, Pasadena, CA, Student Member
[3] Former Postdoctoral Researcher, Caltech, Pasadena, CA now at DLR, Gottingen, Germany.
[4] Professor Emeritus, Caltech, Pasadena, CA, AIAA Fellow
[5] Professor, Caltech, Pasadena, CA

of holes with d=0.5mm, a straight and a saw-tooth slot (0.13 mm in width) and two porous configurations; one continuous and one with discrete plugs. In all these cases the injection flow was normal to the test article surface. The tests were conducted at M=6, 7.3, and 10 with stagnation pressures of 0.87, 10.0, and 13.8 MPa, and stagnation enthalpies of 0.5, 1.1, 2.5 MJ/kg, respectively. It was found that for a given mass flow rate (from about 4.54e-6 to 4.54e-4 kg/s) the continuous porous section and the straight slot were the least efficient to trip the boundary layer while the single row of small holes was among the most efficient configurations. For the single row of 17 of the larger holes, at a ratio of about 20 between the reservoir and the free-stream pressure the trip location moved substantially closer to the inlet. In all cases, choked flow was produced through the orifices or porous media. However, when no flow was injected there was no disturbance to the flow for most or all of the discrete hole configurations. Later Bathel et al. [2] performed NO PLIF measurements of the one row (d=0.5mm) and single (d=0.254 mm) hole configurations at the M=10 conditions. This work provided a qualitative comparison with the results of Berry et al., who had used phosphor thermography for visualization. There were some differences in the estimates of the transition locations between the two visualization techniques. These experiments highlighted the importance of the flow separation region established upstream of the blowing jets. It was postulated that for low flow rates the gas trapped in the separation region, which is heated by virtue of being in the stagnation region, passes around the jets and propagates downstream, convecting with it higher heating loads. However as the flow rate is increased, the jets' cross section becomes larger and the gas from the separation region can no longer pass around the jets; instead the hot gas is forced around the ends of the orifice row. As it passes around the outer jets, it forms a vortex (vortices?) and subsequently distributes the heat downstream.

Another area of interest for tripping mechanisms is transition control. For example, for the shuttle heat shield it is essential to know when in the trajectory the flow will become turbulent. Danehy et al [3] studied boundary layer trips using NO PLIF at the 31 inch Mach 10 wind tunnel at NASA Langley. Their main motivation was to be able to evaluate the consequences of given damage to the shuttle thermal protection system. Rectangular and triangular trips, typically oriented at 45 deg with respect to the flow, were installed on a flat plate. For these trips, k/δ was 0.51, 1.32, and 1.89 for angles of 0, 10 and 20 deg, between the flat plate and the flow, respectively. Their stagnation conditions were P_o=4.96 MPa and T_o=1000K. The Reynolds Number was 3.28e6 per meter. They found that at zero angle of attack the flow remained laminar with both trip geometries. The flow was laminar and transitional at 10 degrees; at 20 degrees the flow was laminar with no trip but turbulent for the two trip geometries.

Recently, Holden et al [5] reviewed experimental programs conducted at CUBRC from the 1970's to early 1990's to examine the effects of blowing and roughness on heating and skin friction on blunt nosetips, slender conical shapes and capsule heat shields. For rough slender cones at M=11, 13, and 15, blowing rates of 0.5 to 4.5 were found to decrease the heating loads and skin friction as compared to a smooth-walled cone. Here the blowing rate is defined as $m/r_e u_e C_{Ho}$. It was also found that surface blowing was more effective in reducing heat transfer than in previous experiments performed at supersonic Mach numbers. At Mach number 11 and Reynolds numbers up to 10e6, roughness elements of 0.38 mm height produced more than double the heat enhancement of 0.254 mm roughness elements as compared to a baseline value of the turbulent heat transfer obtained on a smooth cone.

Work from Korkegi [6] in 1956 showed that for a flat plate at Mach 5.8 with P_o of 0.65 MPa, T_o of 380K and Reynolds number of 8.5e6 per meter, a fully developed turbulent boundary layer is not obtained below Reynolds numbers of 2e6 for normalized air injection rates of up to 4.5%. Here the mass flow rate of the jets per unit span has been normalized by the boundary layer mass defect per unit span. Finally, Coles [7] in 1954 obtained early measurements of the local skin friction over a smooth flat plate at M=4.54 with and without passive trips and air jets. The passive trips consisted of a sand strip and a leading edge fence. The fence consisted of d=0.014" wires, spaced 0.25" apart and projected about 0.10" above the surface of the plate. The air jets consisted of a row of holes with d=0.014", spaced 0.25" apart and positioned 0.75" downstream from the leading edge. At M=4.54 the boundary layer was less sensitive to injection than at lower M values. Coles found that upon crossing a critical value of the mass flow rate, the effect on surface friction was large but did not change appreciably for higher mass flow rates. For M=4.54 the critical value was a decrement of about 25 in the parameter $u_\infty \delta^* / \nu_\infty$ for initial values between 3000 and 5000. Regarding experiments at high enthalpy and the effect of cavities on transition, Germain [8] conducted several experiments with the same geometry used in the current study (sharp 5 degree half-angle cone). In his experiments he created a circumferential gap or cavity at x=0.203 m. The gap was 5 mm deep with 0.127, 0.254, 0.508, and 0.889 mm widths. The test condition was P_o =55MPa and h_o=12 MJ/kg. He observed no significant effects on transition.

In this paper we investigate three injection schemes designed originally to introduce CO_2 into a supersonic boundary layer. The aim of injecting CO_2 is to delay transition at high Mach numbers for slender bodies, as explained in detail in Leyva et al [8]. Briefly, the idea explored in that paper rests on the fact that at high enthalpies CO_2 becomes vibrationally excited and absorbs energy from acoustic disturbances which are responsible for transition in the second or Mack mode. In the process of designing appropriate injection schemes for CO_2, however, we observed that our early injection schemes were in fact effective trips. This paper reports experimental results obtained on the impact of three injections schemes on transition. Two designs consist of discrete injection orifices and one has a porous section instead. The injection schemes were studied as passive trips, with no flow, and as active trips, with CO_2 flow through the orifices or porous section.

II. Experimental Setup

The facility used in all experiments in the current study was the T5 hypervelocity shock tunnel at the California Institute of Technology. It is the fifth in a series of free-piston driven, reflected shock tunnels built by R.J. Stalker, H.G. Hornung and colleagues [1-2]. The T5 facility consists of four major components: the secondary air reservoir (2R), the compression tube (CT), the shock tube (ST), and the test section/dump tank. The first three of these components are illustrated in Figure 1.

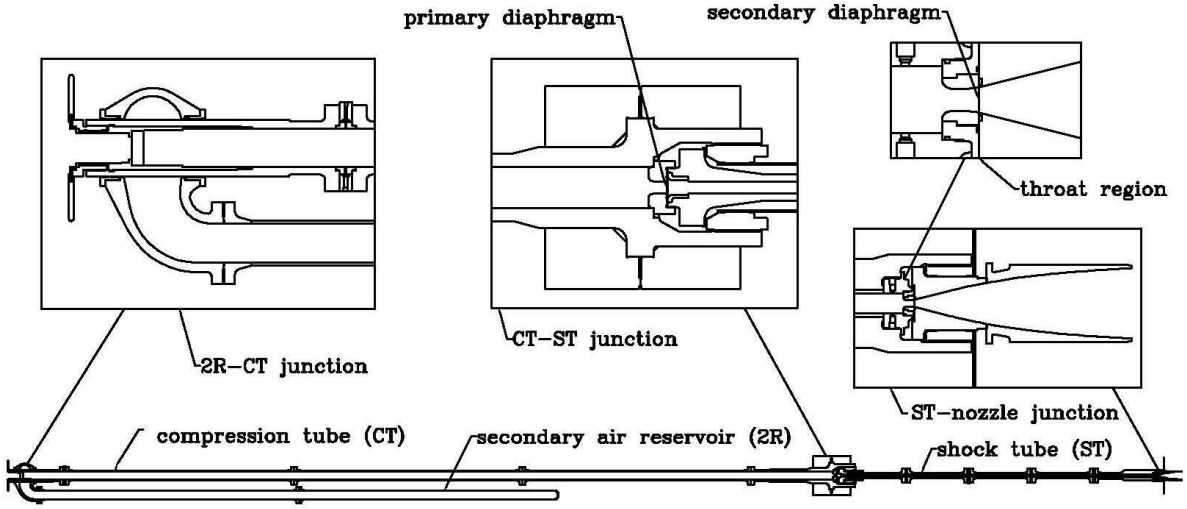

Figure 1. Schematic of the T5 hypervelocity shock tunnel facility.

The test flow is generated by driving a heavy (120 kg) piston down the CT with the release of high-pressure air from the 2R. The CT gas, a mixture of helium and argon, is compressed adiabatically by the advance of the piston until the pressure is sufficiently high to burst the primary diaphragm, located at the junction of the CT and ST. The primary diaphragm typically consists of a 0.187 to 0.270-inch thick stainless steel plate, indented with an X-shaped groove to aid petal formation. The test gas is initially contained in the ST; the burst of the primary diaphragm produces a shock wave that travels the length of the ST and reflects from the end wall. Stagnation conditions are thus produced at the end of the ST, which then serves as the reservoir for the nozzle expansion. The incident shock also bursts the secondary diaphragm, consisting of a 0.002" mylar membrane located at the ST-nozzle junction. The test gas expands through the nozzle, flowing into the test section and finally into the dump tank. The test section and dump tank are initially evacuated, separated from the ST by the secondary diaphragm. Startup of the flow in the test section typically takes 0.5 ms from the time of arrival of the incident shock at the nozzle throat; the test time is of the order of 1-2 ms. In all experiments in the present series, a contoured nozzle of area ratio 100 was used. The initial pressures in the 2R, CT, and ST were typically 5.5-7.6 MPa, 98-116 kPa, and 76-117 kPa, respectively. The test gas for these experiments was air.

The T5 facility is instrumented with various diagnostic tools. An accelerometer attached to the CT is used here to trigger the CO_2 injection when needed. There are also several pressure transducers along the length of the ST. These

transducers are used to measure the incident shock speed and reservoir pressure, from which the flow enthalpy is calculated using the ESTC program, and to trigger the T5 data acquisition system (DAS). The T5 DAS allows simultaneous recording of up to 80 data channels (in addition to the facility data) at a sampling rate of 200 kHz. The T5 optical setup is a typical Z-arrangement Schlieren system, capable of recording either a single frame or a sequence of high-speed images during the test period. A typical exposure time for each frame is 2 μs.

The model employed in the current experiments was a sharp slender cone similar to that used in a number of previous experimental studies in T5. It is a 5 degree half-angle cone of approximately 1m in length and is composed of three sections: a sharp tip fabricated of molybdenum (to withstand the high heat fluxes), a mid-section, and the main body instrumented with 79 thermocouples. These thermocouples have a response time in the order of a few μs and have been successfully used for almost twenty years. For a complete description of the design see Sanderson [11]. The conical model geometry was chosen because of the wealth of experimental and numerical data available with which to compare the results from this program. A photograph of the cone model is shown in Figure 2.

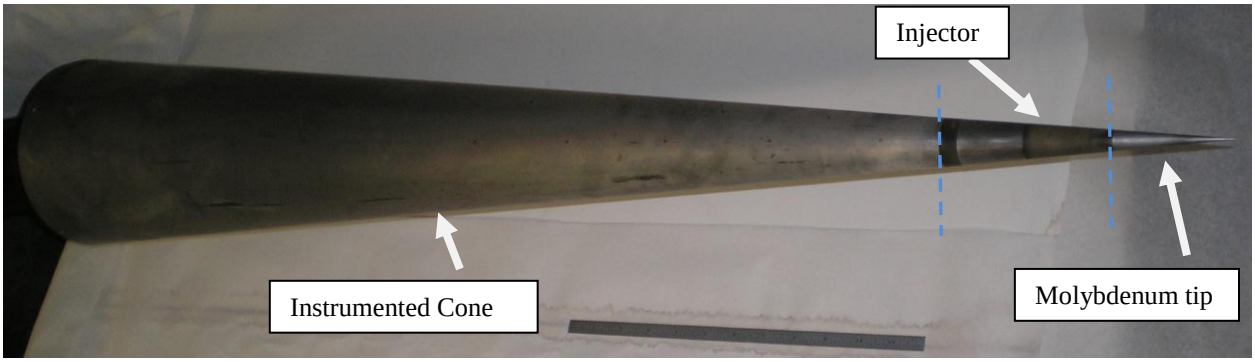

Figure 2. **Cone model used for all experiments. In this case the injector shown is the porous injector.**

III. Experimental Results

A. 4-Row Injector

In these experiments two free-stream conditions were used. Condition A had P_o~51 MPa, h_o~10 MJ/kg, T_o~ 6000K and Condition B had mean values of P_o~44 MPa, h_o~6.5MJ/kg, T_o~4550K. The first injection scheme consisted of 4 rows of injection holes. The diameter of the holes is ~0.76 mm, the minimum diameter which could be reliably manufactured using the chosen technique. These pieces were fabricated using a rapid prototyping technique and the accuracy on the diameter of the holes is not as high as if the holes had been drilled or made using EDM. However, these models were made of a polymer vs. metal which is an advantage because the turnaround time was only a few days, and the cost was much cheaper than regular machining. As an aside, the polymer material survived repeated shots in T5 well, since during the short test times (1-2ms) the cone surface temperature does not rise more than 10 K or so for the conditions used here.

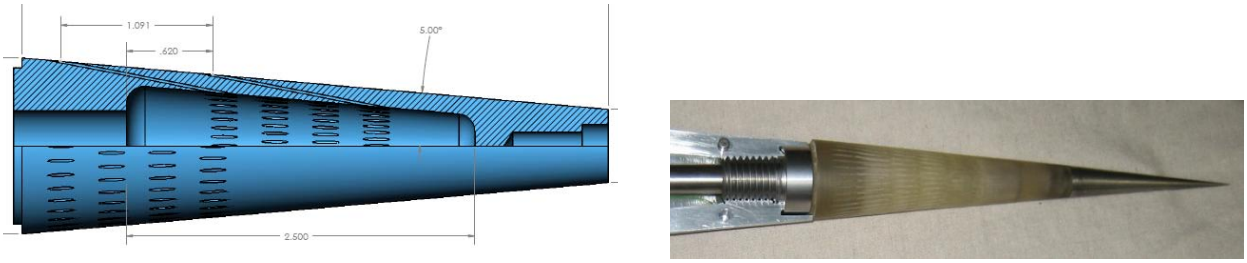

Figure 3. Partial drawing and picture of injector with four rows of holes.

The 4-row injector is shown in Figure 3. The holes were made as close to tangential to the surface as possible; the actual angle between the holes and the surface is 6 degrees. The first row of holes is at 12.9 cm from the tip (along the surface of the cone) and the last row is at 16.5 cm. Each row has 36 orifices. Note that because the holes exit at an angle, the cross sectional area at the exit plane is elliptical. The holes have a length to diameter ratio of about 30. The orifices are connected to a plenum as seen in Figure 3. During a shot this plenum is either under vacuum, if there is no injection or is at a prescribed plenum pressure when injection occurs.

To provide a comparison for the results with the injection schemes, a baseline case was run with a smooth conical midsection (made of the same polymer as the injectors) and the results are shown in Figure 4. Heat flux values are extracted from the 79 temperature readings using the method described in Sanderson [11]. The heat transfer q(x) is then normalized into a Stanton number (St) as follows:

$$St(x) = q(x)/(\rho_e u_e [h_0 - 0.5\, u^2_e(1 - r) - C_p T_w] \quad [1]$$

where r is the recovery factor. For laminar flows, $r_{lam} = \sqrt{Pr}$, and for turbulent flows, $r_{turb} \sim Pr^{1/3}$, where Pr is the Prandtl number. Pr is assumed to be constant, which is a reasonable approximation under the conditions of interest. The Reynolds number is evaluated at the edge conditions, $Re(x) = \rho_e u_e x/\mu_e$. In all the data to be presented here the experimental data is compared with laminar and turbulent heat transfer estimates for a slender cone. An estimate of the location for the onset of transition is obtained by the intersection of the laminar estimate and the line fit obtained from the rising heat transfer points, as indicated in figure 4. In this case natural transition occurs at Re(x)~3.1e6.

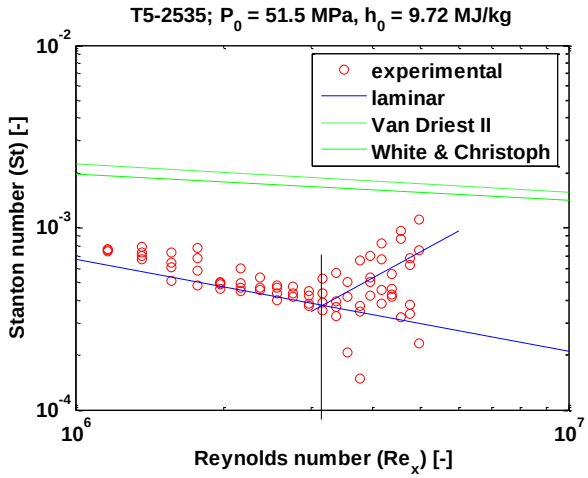

Figure 4. Baseline results with a smooth cone for free-stream condition A.

The results obtained with the 4-row injector are shown in Figure 5. As can been seen in the left plot, the holes induced an early transition by themselves without injection. Transition to fully turbulent values has occurred by the first temperature readings, which are located about 4 cm downstream of the last row of injection holes. Since the holes themselves are sufficient to induce early transition, injection of CO_2 at 0.2MPa, as shown in the right plot, does not change the flow in any appreciable manner. The flow is still fully turbulent as measured by the most upstream thermocouples. Before we obtained the data shown in Figures 4 and 5, we observed a forward facing step between the molybdenum tip and the injector piece. That is, at the junction between the tip and the injector the diameter of the injector was larger than the molybdenum tip by about 0.5 mm. The data obtained with the step is shown in Figure 6. The traces obtained with the step look very similar to the corresponding traces without it. Therefore, the injection holes are sufficient to result on the early transition observed in both figures.

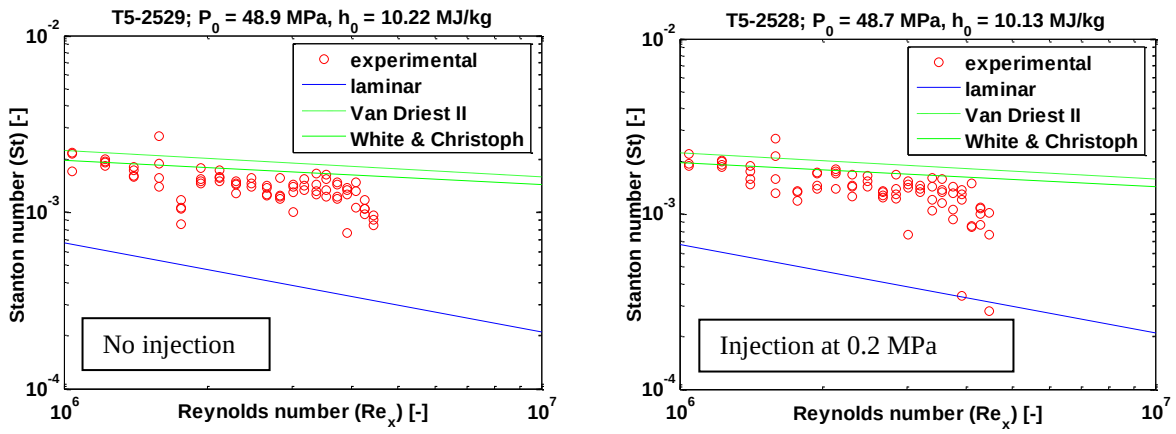

Figure 5. Normalized heat transfer for 4-row injector with and without CO_2 injection.

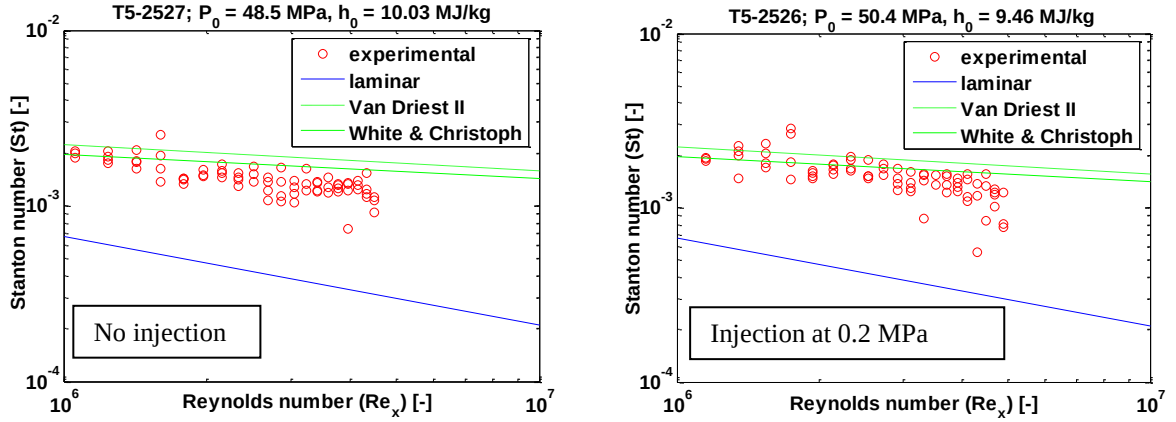

Figure 6. Normalized heat transfer for 4-row injector with and without CO_2 injection with a step between the injector and the molybdenum tip (condition A).

A different free-stream condition was run to assess the effect of the injection holes at a lower stagnation pressure and enthalpy condition (Condition B). As seen in Figure 7, it was found that the smooth cone (left) now has a natural transition point at a Re(x) of about 2.9e6. The case with the 4-row injector (right), with CO_2 injected at 0.2MPa, shows fully turbulent heat transfer values at the most upstream location at which the temperature is measured, 22 cm from the tip. However, one should be cautious to interpret these results since in order to visualize the flow; the cone had to be moved downstream so the injection piece was aligned with the T5 windows. In the new location, the expansion fan from the nozzle is incident upon the back of the cone, which may explain the lower heating values observed at the highest Re numbers. In this position the results are not meaningful for transition location measurements. However, it is likely that the flow would have transitioned even if the cone were in the regular position (upstream). A visualization of the flow during the test time is shown in Figure 8. The visualizations allow one to obtain a sense of the injection process. The left picture in Figure 8 shows injection into vacuum and one can see the expansion fans from the jets. During the test time (right) weak shocks are visible originating from each row of holes.

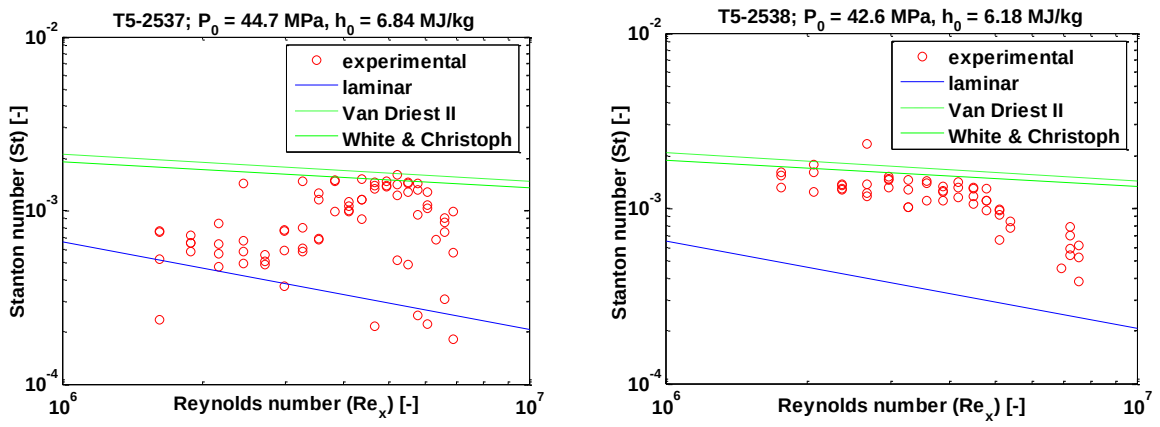

Figure 7. Normalized heat transfer for a smooth cone (left) and a 4-row injector (right) with 0.2 MPa injection pressure (condition B).

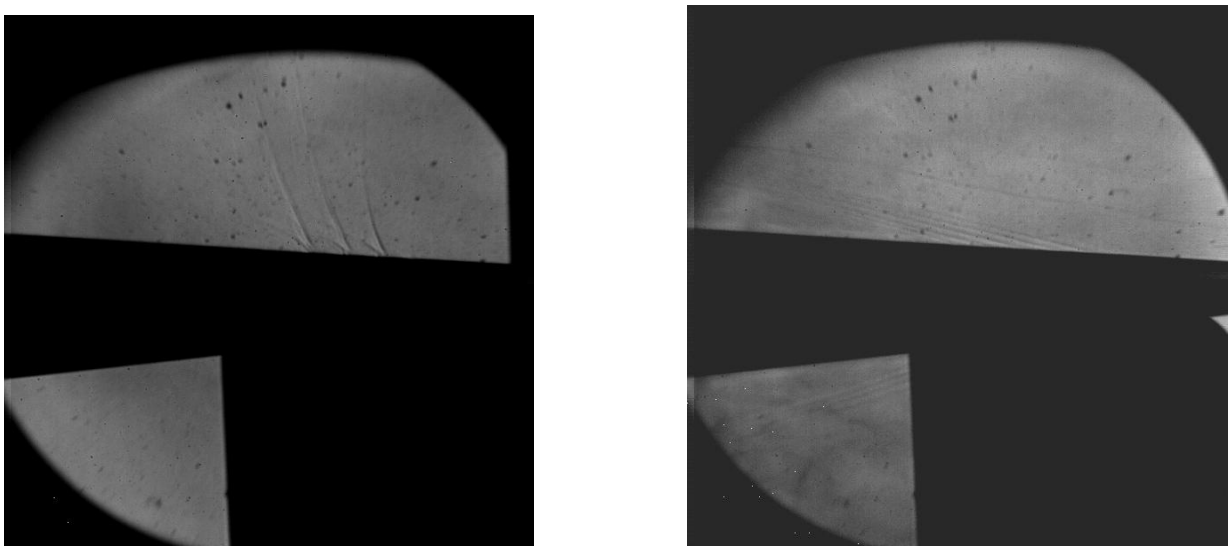

Figure 8. Visualization of flow field with 4-row injector injecting into vacuum (left) and with 0.2MPa injection pressure during shot 2538 (Figure 7 right).

B. 1-Row Injector

To decrease the impact of the holes on transition, a new injector was built with only one row of holes. The design basically consisted of the previous injector with only the last row of holes. This injector was tested at condition A and the results are shown in Figure 9. When compared to the baseline case with a fully smooth cone (shot 2535, shown in Figure 4) the transition onset is seen to have been moved forward to a Re(x) of about 2e6. Thus, though the transition was not accomplished within 4 cm from the last injection row, as with the 4-row injector, it was still moved upstream significantly.

As has been seen from the previous cases for both the 1-row and the 4-row injectors, the tangential orifices are very effective at promoting transitions at the conditions studied. A rough estimate of the boundary layer height at the location of the first row of holes is between 0.5 to 0.7 mm, which makes the ratio of the orifice diameter to the boundary layer height approximately 1 to 1.5. One possible explanation for the way in which the holes induce

transition is through the wake mode discussed in Rowley et al. [7]. This mode is observed in longer cavities (with respect to the boundary layer thickness) and higher Mach numbers compared to the Rositter or shear layer mode which is observed for shorter cavities and lower Mach numbers. The wake mode is characterized by a large-scale vortex shedding, in which a Kelvin-Helmholtz instability grows and produces a strong recirculation flow in the cavity. The flow is absolutely unstable and the Strouhal number is independent of Mach number [7]. Further studies would be needed to confirm this idea.

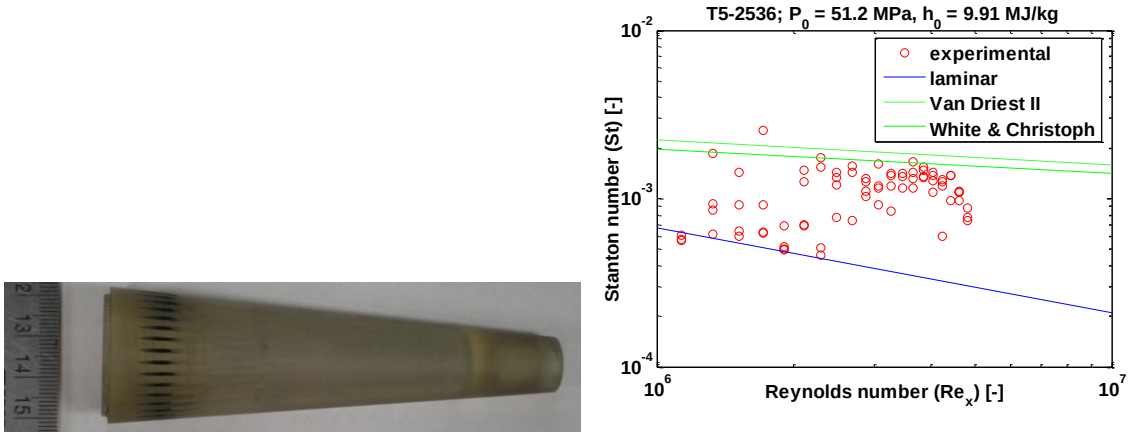

Figure 9. Left: 1-Row injector design. Right: Normalized heat transfer for the 1-row injector with no injection.

C. Porous Injector

A porous injector was designed with the purpose of achieving a more spatially uniform injection flow, similar to transpiration cooling, instead of the discrete jets created with the designs discussed earlier. The piece chosen has 10μm porosity and is fabricated from sintered stainless steel [8]. The manufactured injector is shown in Figure 10. Porous injector. The thickness of the porous media is about 2 mm. It starts at 12.8 cm from the tip and is 41 mm in length.

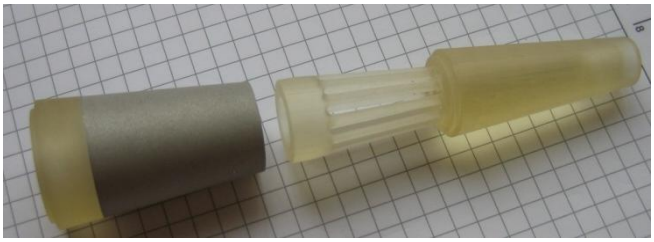

Figure 10. Porous injector.

Results for this geometry are shown in Figure 11. The free-stream conditions are similar to those of shot 2535 presented in Figure 4. The fact that the transition Reynolds numbers are very similar in the two cases indicates that the porous material does not itself cause transition. This is in contrast with the previous injector designs. A run was also conducted for the purpose of visualizing the injection of CO_2 through the porous material. Again, the cone was moved backward so that we could visualize the injector section. The results are presented in Figure 12. The CO_2 flow is evident in frames b-e. It is worth pointing out that a Schlieren setup is sufficiently sensitive to visualize the CO_2 injection process, which means more complex visualization techniques are not required. There is a shock emanating from the interface between the molybdenum tip and the injector due to a small discontinuity which was

smoothed out prior to the following shot (2540). The heat transfer traces show transition to fully turbulent flow by the third or fourth thermocouple location. This is the only case studied in which injection was necessary to produce early transition. If the aim is to delay transition, as in the present case, it seems the injection pressure should be kept lower than 0.55 MPa. With this in mind, a preliminary shot was conducted with CO_2 injection at 0.2MPa and it appeared that the transition Reynolds number was not affected as compared to the smooth case. This condition as well as other conditions with higher injection pressures will be completed in the next couple of months to find the practical range of CO_2 supply pressures which do not result in early transition.

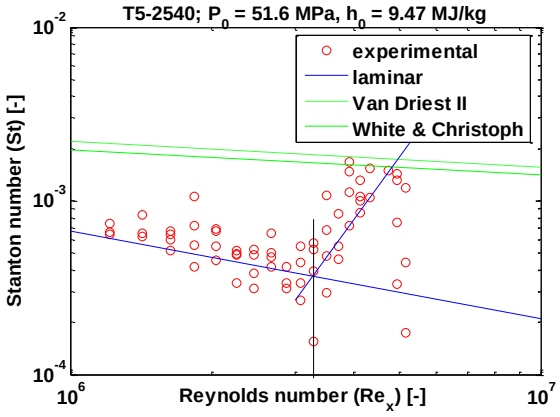

Figure 11. Normalized heat transfer for porous injector with no injection.

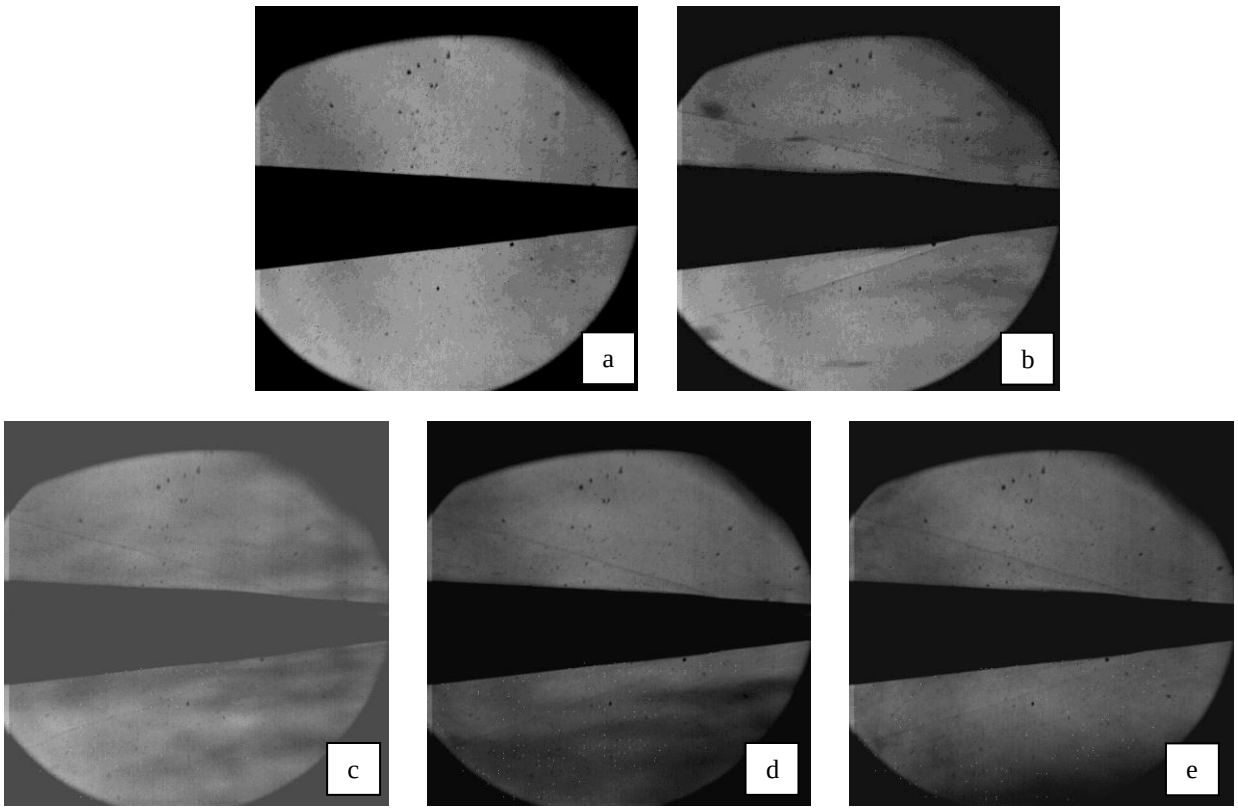

Figure 12. Shot 2539. Consecutive frames of a high-speed movie of the flow over the cone with the porous injector and 0.55 MPa CO_2 injection . The stagnation conditions were P_o=52 MPa and h_o=9.7MJ/kg.

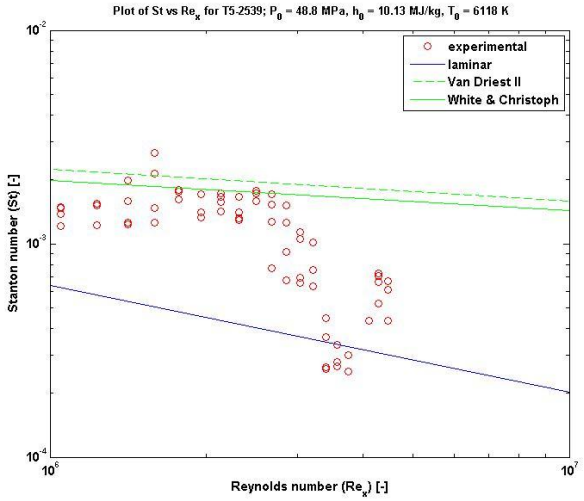

Figure 13. Normalized heat transfer for Shot 2539 with the porous injector and 0.55 MPa CO_2 injection.

IV. Conclusion

Three injection schemes were studied both as passive trips with no injection and as active trips with CO_2 injection. The first design had four rows of 36 orifices with diameters of 0.76 mm. The second injector was derived from the former one by only keeping the fourth or most downstream row of orifices. The third injector consisted of a section with 10 μm porousity. The 4-row injector tripped the boundary layer to fully turbulent values within 4 cm from the last row of orifices for the two free-stream conditions studied. The transition Reynolds number with the 1-row injector was decreased by about 50% as compared to the smooth cone. Therefore, while not as efficient as the 4-row injector, one row of holes still caused early transition. The 4-row injector was also tested with CO_2 injection pressure of 0.2MPa but the injection did not change the experimental results obtained. A porous injector was also tested and did not result in early transition when tested without injection. Injecting CO_2 at 0.55 MPa through the porous media seemed to cause early transition.

Acknowledgments

The authors would like to thank Bahram Valiferdowsi for helping with the design of the injection pieces and with the maintenance of the facility. Financial support for this work was provided in part by the Air Force Office of Scientific Research, USAF, under grant/contract number F49620-IHOUSE07E0000. The program manager is Dr. John Schmisseur to whom the authors are grateful for his continued support throughout this project.

References

1 Berry, S. A., Nowak, R. J., Horvath, T. J., "Boundary Layer Control for Hypersonic Airbreathing Vehicles", AIAA 2004-2246.

2 Bathel, B.F., Danehy, P.M., Inman J.A., Alderfer, D.W., Berry, S.A., "PLIF Visualization of Active Control of Hypersonic Boundary Layers Using Blowing", AIAA 2008-4266.

3 Danehy, P.M., Garcia, A. P., Borg, S., Dyakonov, A.A., Berry, S.A., (Wilkes) Inman J.A., Alderfer, D.W., "Fluorescence Visualization of Hypersonic Flow Past Triangular and Rectangular Boundary-Layer Trips", AIAA 2007-536.

4 Berry, S.A., Auslender, A.H., Dilley, A.D., Calleja, J.F., "Hypersonic Boundary Layer Development for Hyper-X", *J. Spacecraft and Rockets*, Vol. 38, No. 6, pp. 853-864, 2001.
5 Holden, M.S., Mundy, E.P., Wadhams, T.P., "A Review of Experimental Studies of Surface Roughness and Blowing on the Heat Transfer and Skin Friction to Nosetips and Slender Cones in High Mach Number Flows", AIAA 2008-3907.
6 Korkegi, R., H., "Transition Studies and Skin-Friction Measurements on an Insulated Flat Plate at a Mach Number of 5.8", *J. of the Aeronautical Sciences*, Vol. 23, No. 2, February 1956.
7 Coles, D., "Measurements of Turbulent Friction on a Smooth Flat Plate in Supersonic Flow", *J. of the Aeronautical Sciences*, Vol. 21, No. 7, July 1954.
8 Germain, P., "The Boundary Layer on a Sharp Cone in High-Enthalpy Flow", GALCIT, Caltech, Ph.D. thesis, 1994.
9 Leyva, I.A., Laurence, S., War-Kei Beierholm A., Hornung H.G., Wagnild R., Candler, G., "Transition delay in hypervelocity boundary layers by means of CO2/acoustic instability interactions", AIAA 2009-1287
1 Hornung, H., Belanger, J., "Role and techniques of ground testing simulation of flows up to orbital speeds", AIAA 90-1377.
2 Hornung, H., "Performance data of the new free-piston shock tunnel at GALCIT", AIAA 92-3943.
3 Sanderson, S., "Shock Wave Interaction in Hypervelocity Flow", GALCIT, Caltech, Ph.D. thesis, 1995.
4 Murphy, K.J., Borg, S.E., Watkins, A. N., Cole, D. R., Schwartz, R. J., "Testing of the Crew Exploration Vehicle in NASA Langley's Unitary Plan Wind Tunnel", AIAA 2007-1005.
5 Udovidchik, N., Morrison, J.F., "Investigation of Active Dimple Actuators for Separation Control", AIAA 2006-3190.
6 Thyson, N., Todisco, A., Reeves, B., McCauley, W.D., "Active and Passive Tripping of Frustum Transition at Mach Numbers of 8 and 10", AIAA 1978-1128.
7 Rowley. C. W., Colonius, T., Basu, A. J., "On self-sustained oscillations in two-dimensional compressible flow over rectangular cavities", *J. Fluid Mech.*, Vol. 455, pp. 315-346, 2002.
8 http://www.mottcorp.com/sitemap/sitemap.htm